

RFQ Linac and its limit and Problem

Bosi Wang Oct. 13, 87

Outline

- Introduction
- Para-axial field
- Beam Dynamics
- RF structure
- Limit and problem

1. Introduction

In the 50's the rf quadrupoles had been used for focusing of charged particle beam and rf massspectrography.

(J. P. Blewett, Phys. Rev. 88, 1197 (1952))

(W. Paul et.al., Z. Physik 140 (1955))

In their cases only the two dimensional field had been used (no longitudinal variation)

(3)

that is only the following field

$$u(r, \varphi) = \frac{1}{2} V \sum_{s=0}^{\infty} A_{os} r^{2(s+1)} \cos 2(s+1)\varphi \quad (1.1)$$

had been used.

The contribution of I. M. Kapchinskij and V. A. Teplyakov is that they introduced three dimensional field

$$u(r, \varphi, z) = -\frac{V}{2} \left[\sum_{s=0}^{\infty} A_{os} r^{2(s+1)} \cos 2(s+1)\varphi + \right. \\ \left. \sum_{n=1}^{\infty} \sum_{s=0}^{\infty} A_{ns} I_{zs}(knr) \cos 2s\varphi \sin knz \right] \quad (1.2)$$

The first term in (1.2) is pure two-dimensional multipole field. The second one in (1.2) gives longitudinal field component E_z .

The contribution of Los-Alamos group is that they simplified the field expression of (1.2) and only took two lowest order term:

$$U_0(r, \varphi, z) = -\frac{V}{2} [A_{00} r^2 \cos 2\varphi + A_{10} I_0(kr) \sin kz] \quad (1.3)$$

Using (1.3) if the shape of vane is a perfect hyperbol cross-section you will have the precise field distribution determined by (1.3).

And the Los Alamos group built first prototype of RFQ Linac with high transmission efficiency ($> 90\%$), and they wrote a series of computer programs for beam dynamics design.

Soon after that it had found that the tolerance of the intervane voltage is very tight

$$\frac{\delta V}{V} = -\frac{1}{6} \frac{L^2}{\lambda^2} \frac{\delta C}{C} \quad (1.4)$$

$$\frac{\delta C}{C} \approx -\frac{\delta f}{g} \quad (1.5)$$

where V — intervane voltage

δV — deviation of V

L — the total length of the RFQ Linac

λ — rf wave deviated by 2π

C — capacitance between adjacent vanes

g — the average intervane gap

δC — the deviation of C

δg — the deviation of g

Example : if you want to keep $\frac{\delta V}{V} \lesssim 10\%$

($L \approx 3 \text{ m}$, $f = 425 \text{ MHz}$) the $\delta g \lesssim 0.003 \text{ mm}$.

(D. D. Armstrong. et. al. RFQ Devel. At Los Alamos)

Field stabilization is important.

First at Los Alamos used manifold (J.M. Potter
1979 Linear Acc. Conf.)

Then several RFQ structures had been proposed,
but at present two of them are more successful
than others. They are

- vane coupling rings (VCR)

- (Proposed by H. Lancaster et. al. 12th Int. Acc.
Conf., FNAL, P. 512 (1983))

- Resonant Loop Coupling (RLC)

(Proposed by A. Schempp. 1986 Linear Acc.

Conf. P. 251, SLAC (1986))

2. Para-axial field

If you look around the axis in RFQ cavity
the field near axis can be described by Laplace
equation (quasisteady state)

$$\frac{\partial}{\partial r} \left(r \frac{\partial \phi}{\partial r} \right) + \frac{1}{r} \frac{\partial^2 \phi}{\partial \theta^2} + r \frac{\partial^2 \phi}{\partial z^2} = 0 \quad (2.1)$$

The general solution is

$$\phi = e^{\pm jkz} \frac{\cos n\theta}{\sin n\theta} [C_1 J_n(PkR) + C_2 N_n(PkR)] \quad (2.2)$$

$$C_2 = 0 \quad \because r \rightarrow 0, N_n(0) \rightarrow -\infty$$

if we have ^asine form modulation along z axis
PK should be imaginary $Pk \rightarrow jpk$ So Bessel

function $J_n(PK\varphi)$ is changed into modified

$$J_n(jPK\varphi) = j^P I_n(PK\varphi) \quad (2.3)$$

$$\phi = \sin PK\varphi \frac{\cos n\varphi}{\sin n\varphi} C_1 I_n(PK\varphi) \quad (2.4)$$

And if chose the symmetric plane of multipole as the initial reference plane then (2.4) can be written as

$$\phi = C_1 \sin PK\varphi \cos n\varphi I_n(PK\varphi) \quad (2.5)$$

For the property of symmetry of the multipole (including quadrupole) n should be even

$$\phi_1 = C_1 \sin PK\varphi \cos 2S\varphi I_{2S}(PK\varphi) \quad (2.6)$$

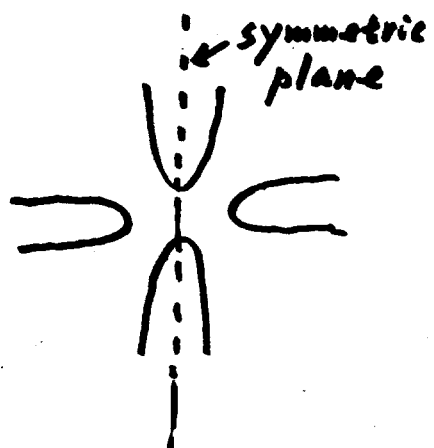
If the $K=0$ the field is two-dimensional

$$\frac{\partial^2 \phi}{\partial r^2} + \frac{1}{r} \frac{\partial \phi}{\partial r} + \frac{1}{r^2} \frac{\partial^2 \phi}{\partial \varphi^2} = 0 \quad (2.7)$$

Because the quadrupole has to be included

and we have taken symmetrical plane as initial reference plane the solution for (2.7) is

$$\phi_2(r, \theta) = \sum_{s=0}^{\infty} A_{0s} r^{2(s+1)} \cos 2(s+1)\theta \quad (2.8)$$



The general form of (2.6) can be written as

$$\phi_1 = \sum_{p=1}^{\infty} \sum_{s=0}^{\infty} A_{ps} I_{2s}(PKr) \cos 2s\theta \sin PKz \quad (2.9)$$

Superposition of ϕ_1 and ϕ_2 is

$$\phi = \sum_{s=0}^{\infty} A_{0s} r^{2(s+1)} \cos 2(s+1)\theta + \sum_{p=1}^{\infty} \sum_{s=0}^{\infty} A_{ps} I_{2s}(PKr) \cos 2s\theta \cdot \sin PKz$$

According to (2.10) we have following field components :

A_{10} — axial symmetric field

A_{00}, A_{11} — quadrupole

A_{12} — (8 pole) Octapole

A_{13}, A_{01} - (12-pole) Duosixapole

A_{14} - (16-pole) ? (how to call in english)

A_{02} - (20-pole) Duodesimal

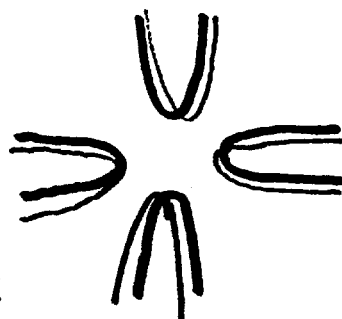
:

This is the ideal case in which the four electrodes (whatever geometric shape they have) are exact symmetric around the axis. In practice the four electrodes can not be assembled so precisely. So in general case the dipole, sextapole, 10-pole, 14-pole ... are also exist

$$A_n \left(\frac{r}{r_0}\right)^n \cos n\vartheta \quad (2.11)$$

$$n = 0, 1, 2, 3, \dots$$

the blue one is ideal case



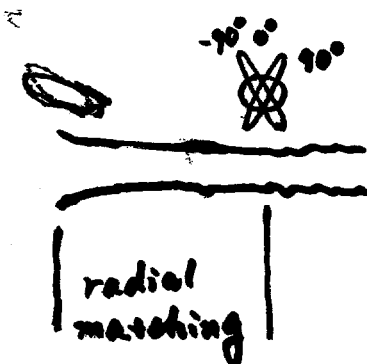
the red one is non-ideal case

3. Beam dynamics

Two points have to be noticed

- ① From time independent acceptance to time dependent (rf) acceptance.

How to match?



First chose radius ^{of aperture} at the end of radial matching section and give the emittance from the ion source to determine the shape of acceptance ellipses relative to different rf field phases (-90°, 0°, 90°, 180°...). Then trace these ellipses back to the input (5-10 perellipses)

Because the strength of field $B = \frac{e\lambda^2}{m_e c^2} \frac{XV}{a^2}$

is decreasing toward the input. So the three ellipses at the input have small difference.

- ② The transverse and longitudinal current limits are determined at the end of gental bunches. This is because at the end of gental bunches $\varphi_s = -35^\circ -- 30^\circ$ that is almost the final synchronous phase. The angular length of the separatrix Φ is determined by

$$\tan \varphi_s = \frac{\sin \Phi - \underline{\Phi}}{1 - \cos \underline{\Phi}} \quad (3.1)$$

and the bunch space length $\sqrt{s_b}$ is :

$$z_b = \frac{\beta \lambda \Phi}{2\pi} \quad (3.2)$$

From (3.1) and (3.2) it is obvious that at the end of gental buncher

is the minimum (which is kept constant through the acceleration section) and the space charge density is the maximum. According to the formulae (smooth approximation T. P. Wangler)

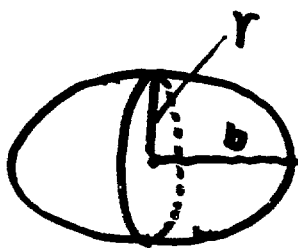
$$I_t = \frac{4 M_t m_e c^2 \rho \delta^3 |\phi_s| \sigma_0^2}{32 \cdot e \gamma N^2 \psi [1 - f(p)]} \left(\frac{q}{\lambda} \right)^2 \quad (3.3)$$

where M_t — ratio of transverse space charge force to focusing force
 σ_0 — phase advance at zero current
 N — ratio of number of focusing period per $\beta\lambda$
 $f(p)$ — space charge form factor

$$I_l = \frac{8\pi^2}{32} M_l \frac{r^2 b}{f(p)} \frac{1}{\rho \lambda^2} E_0 T | \sin \phi_s | \quad (3.4)$$

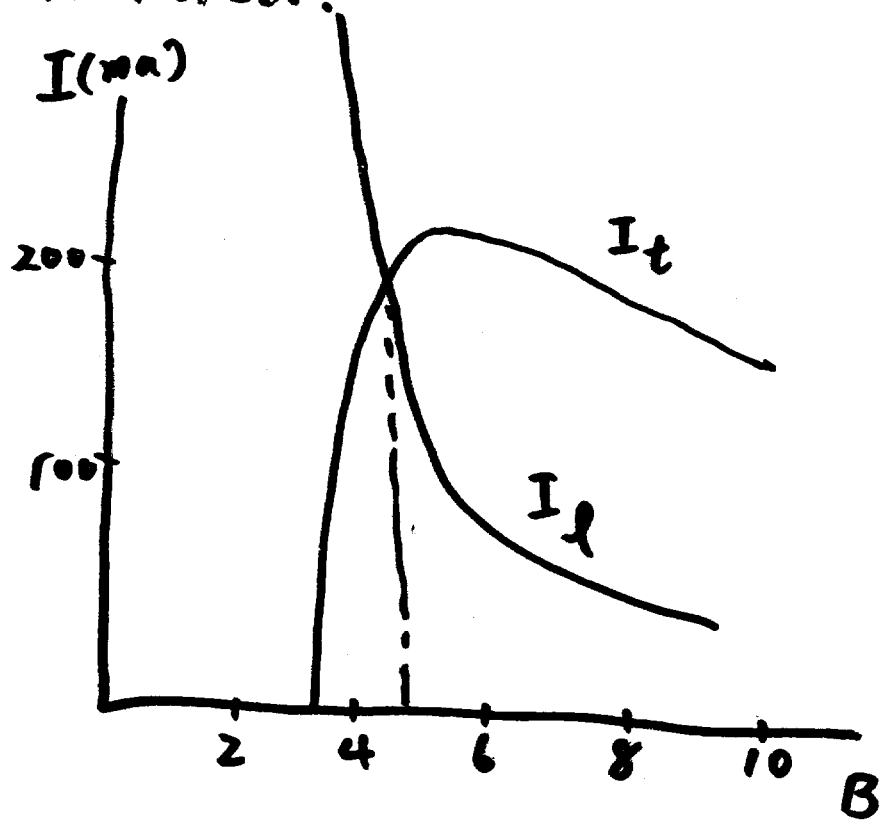
where M_l — ratio of longitudinal space charge force to the focusing force

for space charge the ellipsoid model is used



Suppose bunch has a ellipsoidal shape.

then the I_t (trans. space charge limit current) and I_L (longitudinal sp. ch. limit current) are calculated.



4. RF Structure

According to the frequency RF structure can be devived into two categories:

a) High frequency

Four vane structure which itself involves many substructures: (See Table 1)

VCR — Vane Coupling Rings (Lancaster, 1983)

RLR — Resonant Loop Rings (Schempp, 1986)

DDR — Double Dipole Resonator (Hutcheon, 1982)

AHS — Alternating Half Short (Hutcheon, 1982)

(B. Wang, 1981)

The above listed structures are for transverse field stabilization.

There are very few works on the longitudinal field stabilization:

RLC — Resonant Line Coupling (Schempp 1986)

3-D VCR — three dimensional Vane coupling rings
 (proposed by
 B. Wang 1987)

b) Low frequency RFQ Structures

Split Coaxial Resonator

Four Rod straight stems (Frankfurt Uni.)
 spiral (and Chalk River)

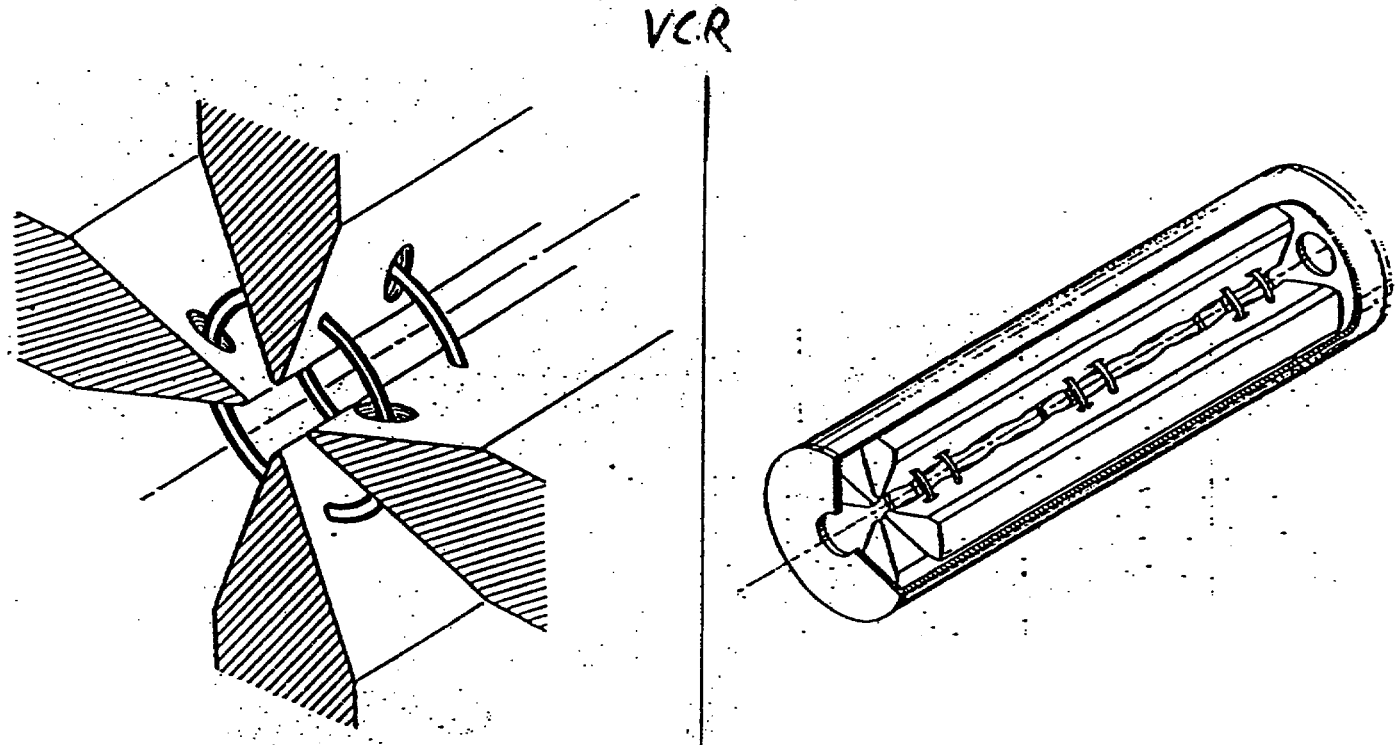
Double - H type Resonator (for high frequency)
 (first by Soviet Union)

Low frequency structure is used for
 heavy ion acceleration (β is low)

Comparison between 4-rod and 4-vane
 structure (201.25 MHz)

- ① In principle rf power loss in 4-vane cavity smaller than that in 4-rod stem structure.
- ② 4-rod use trapezoidal shape to increase accelerating efficiency $\approx 10\%$, so the net rf efficiency may be the same as for the four vane structure. But 4-vane can also use trapezoidal shape tip. Then 4-vane structure will have higher rf efficiency than 4-rod structure.
- ③ 4-rod structure is simpler than 4-vane structure.

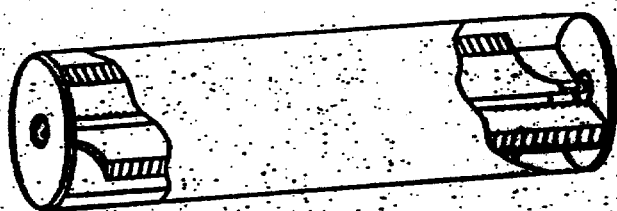
* VANE COUPLING RINGS (VCRs): STABILIZES INTERNALLY THE 4-V STRUCTURE, SO THE CAVITY CAN BE LOOP-DRIVEN INSTEAD OF MANIFOLD-DRIVEN. THE VCRs ELIMINATE THE DIPOLE MODES IN THE FREQUENCY RANGE OF INTEREST, PROVIDE ADEQUATE QUADRANT BALANCE AND SIMPLIFY END TUNERS, BUT THE FREQUENCY OF THE FUNDAMENTAL RFQ MODE IS SHIFTED BY A FEW PERCENT TO A LOWER VALUE BY THE VCR'S.



* ALTERNATING HALF SHORT STRUCTURE OR FOLDED DIPOLE (WANG BO-SI DESIGN)

3522

AHS



(a)

DDR

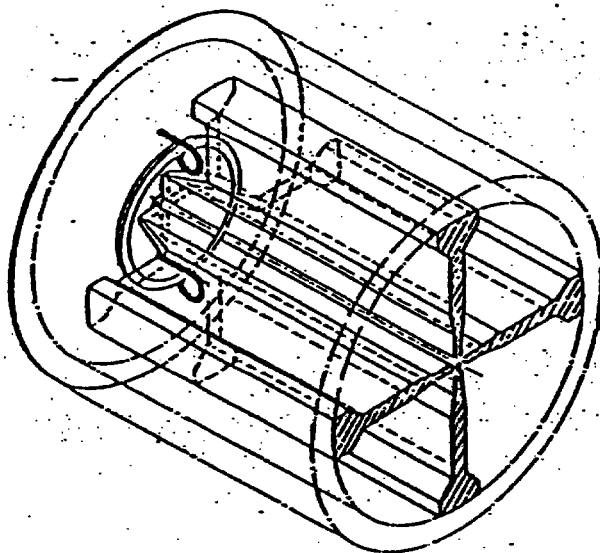


(b)

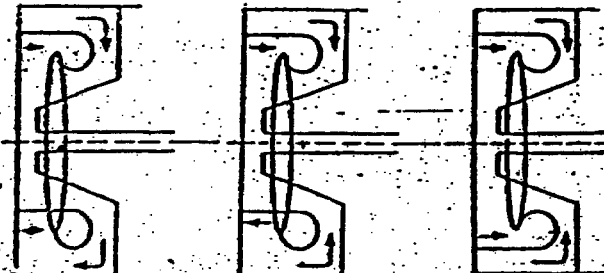
Cutaway diagrams showing two new end termination configurations which increase field stabilities
- (a) folded dipole, (b) one half of a double dipole.

* RESONANT LOOP RINGS (RLR)

RLR



End cell resonant loop ring (RLR)
coupler scheme



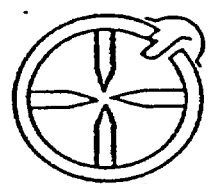
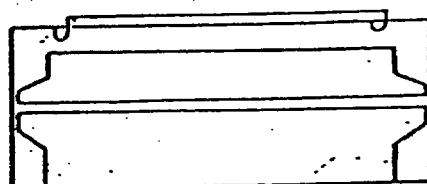
Dipole

Quadrupole

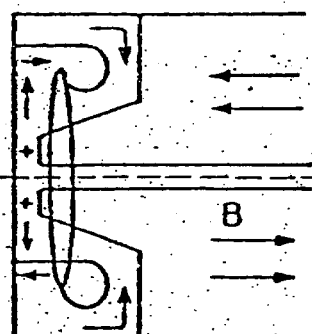
Quadrupole-Mode

End cell excitation of an RLR

RLC



Set-up for longitudinal stabilisation
with one RLC



End cell resonant coupler

⑩ Table 1

TABLE OF RFQ LINAC STRUCTURE

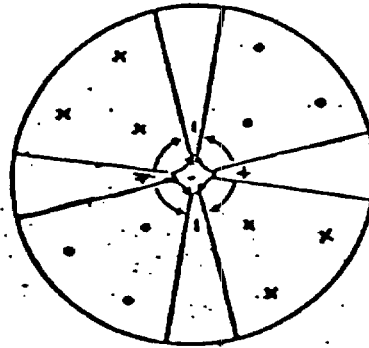
STRUCTURES FOR AZIMUTHAL FIELD STABILIZATION

NAME OF STRUCTURE	VCR	RLR	DDR	AHS
FEATURE OF STRUCTURE	Shorting open site vanes by conductor rings	Inserting a con- ductor ring with two diameterly placed loops into vane end nose	Connecting two resonators of T_{M01} -like mode	Alternatively shorting two pairs of opposite vanes to cavity end walls
OPERATING MODE	disturbed $\frac{I}{2}$ mode	disturbed $\frac{I}{2}$ mode	π	zero
COUPLING BETWEEN QUADRANTS	Stronger than ordinary RFQ	Stronger than ordinary RFQ	Weaker than ordinary RFQ	approximately two times larger than ordinary RFQ
MODE SEPARATION	larger than ordinary RFQ	larger than ordinary RFQ	larger than ordinary RFQ	larger than ordinary RFQ
GROUP VELOCITY AZIMUTH	small	small	zero	zero
AUTHORS	Berkeley group, LISA West Germany	Frankfurt University Canada	Chalk River Nud. Lab. Canada	IHEP, China TAC, USA Chalk River Nud. Lab.

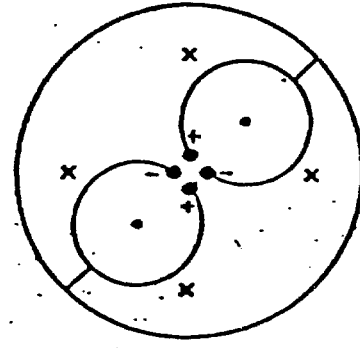
Table 2

STRUCTURE FOR LONGITUDINAL FIELD STABILIZATION

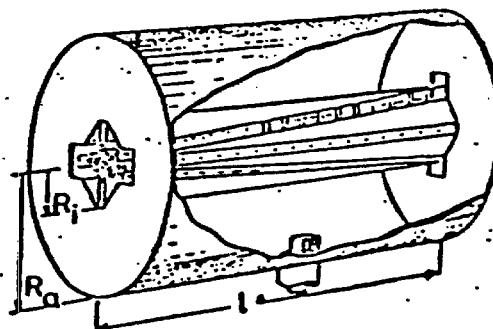
NAME OF STRUCTURE	RLC	3-D VCR*
FEATURE OF STRUCTURE	Similar to RLR	Connecting of opposite vanes by inclined rings
OPERATING MODE	?	$\frac{\pi}{2}$ for both azimuthal and longitudinal
COPPLING IN LONGITU- DINAL DIREC- TION	Larger than without RLC	Large in both azimuthal and longitudinal directions
MODE SE- PARATION	Larger than without RLC	Large in both azimuthal and longitudinal directions
GROUP VELOCITY LONGITUDINAL	highest for both azimuthal and longitudinal	Shimming of vane edge or end tuning) only in static state but not in dynamic state.
AUTHORS	Frankfurt Univ.	TAC group *no experiment factor RFQ Linacs.



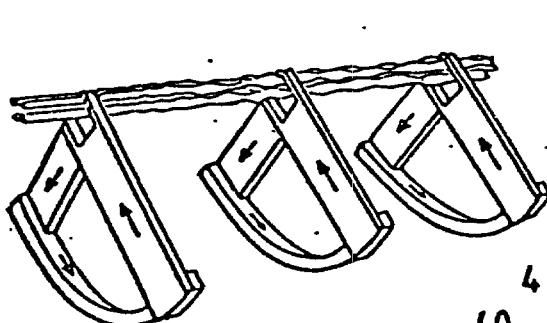
Four Vane Resonator
(TE_{210} -like)



Double - H - Resonator
($2 \cdot TE_{110}$ -like)

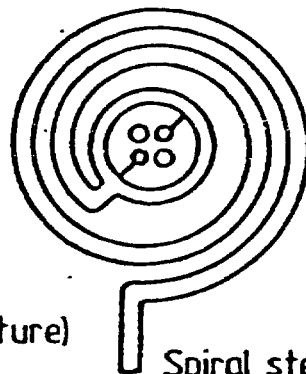


Split Coaxial Resonator (TEM-like)

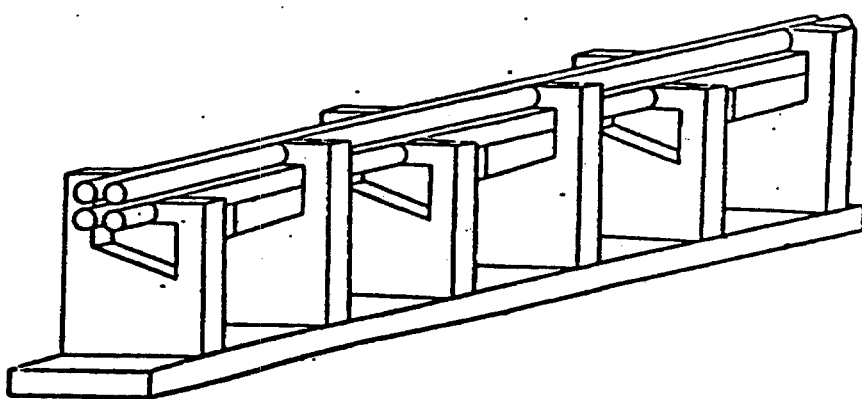


Straight stems

4 - ROD - RFQ
(0 - Mode - $\lambda/2$ structure)



Spiral stems



Linear · 4 - ROD - RFQ

(2)

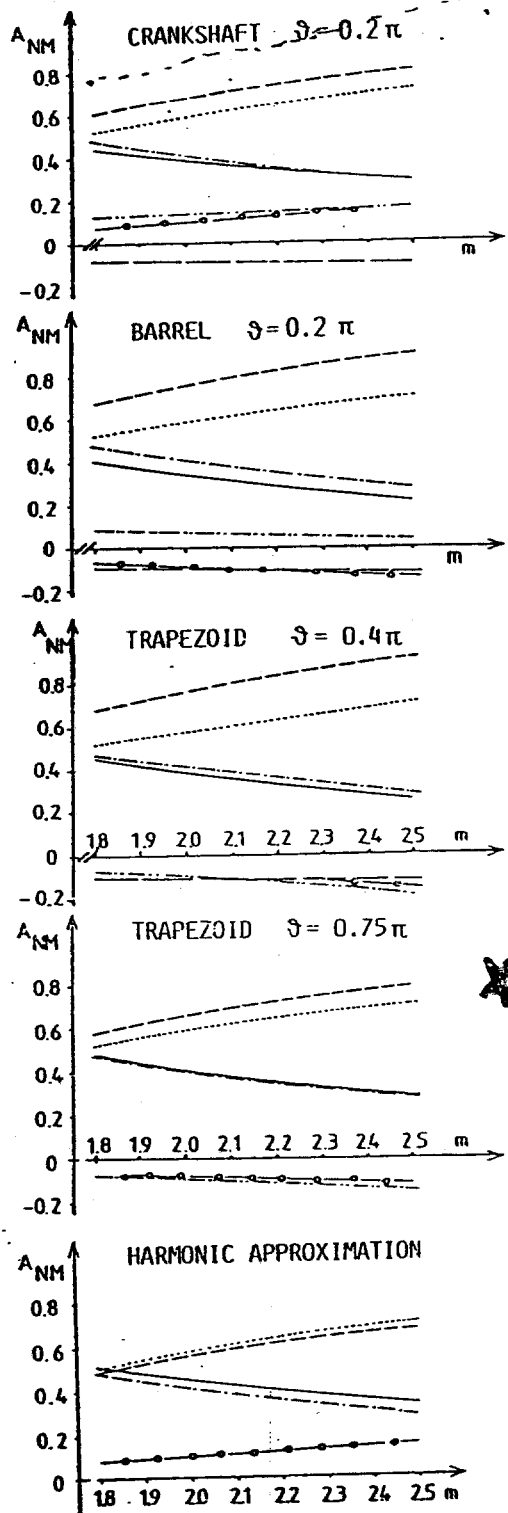


Fig. 5 Field harmonics A_{NM} of representative section with $ka = 0.274$ versus modulation ($a = 3$ mm, 108 MHz, 300 keV proton energy)

— A_{10} , ideal A_{10} ,
— A_{01} , ideal A_{01} , — A_{12} ,
— A_{21} , — A_{30}

Normalization $A_{01} = A_{01}/a^2$

$$A_{NM} = A_{NM}/I_{2M} \left(\frac{Nk^2 + b}{2} \right)$$

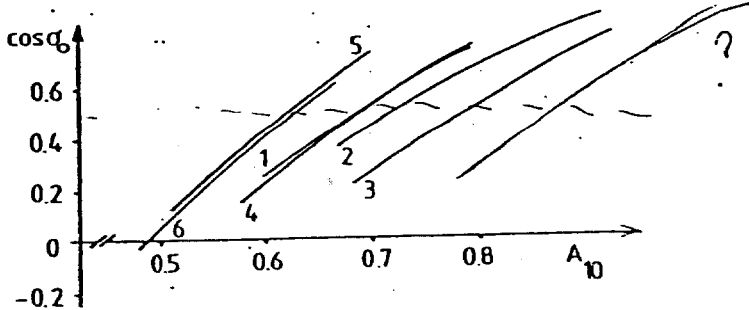


Fig. 6 $\cos\theta_0$ versus A_{10} of figs. 5, electrode voltage 30 kV
1 crankshaft, 2 barrel, 3 trapezoid
 $\theta = 0.4\pi$, 4 trapezoid $\theta = 0.75\pi$, 5 ideal,
6 approximation of 5

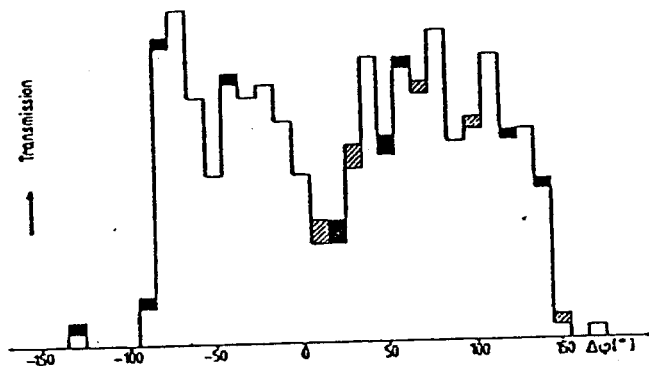


Fig. 7 Gains ■■■ and losses ▒▒▒ of particles due to A_{21} in proton linac^{3,4,5}. Transmission about 6 mA, shaper omitted in design, PARMTEQ code, transmission versus phase plotted.

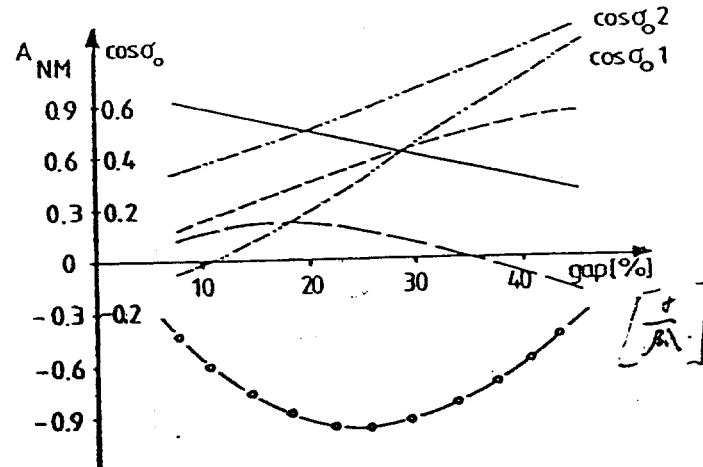


Fig. 8 Field harmonics of fingers type 4 with $ka = 0.274$ and $\cos\theta_0$ versus gap in % of 8λ , $a = 6$ mm, 13.5 MHz, 18.75 keV/amu energy, $\cos\theta_0$ corresponding to 1. 120 kV for ions with $q/\text{amu} = 1/130$ resp. 2. 150 kV, 1/208 Legend of curves as in fig. 5

5. Limit and Problem

If we look at two term potential field

$$U = \frac{V}{2} \left[X \left(\frac{r}{a} \right)^2 \cos 2\vartheta + A I_0(Kr) \cos Kz \right] \quad (5.1)$$

$$E_r = -\frac{XV}{a^2} r \cos 2\vartheta - \frac{KAV}{2} I_0(Kr) \cos Kz \quad (5.2)$$

$$E_\vartheta = \frac{XV}{a^2} r \sin 2\vartheta \quad (5.3)$$

$$E_z = \frac{KAV}{2} I_0(Kr) \sin Kz \quad (5.4)$$

$$A = \frac{m^2 - 1}{m^2 I_0(Ka) + I_0(mKa)} \quad (5.5)$$

$$X = 1 - A I_0(Ka) \quad (5.6)$$

In a design of RFQ A should increase so $m \rightarrow$ increase, $X \rightarrow$ decrease

A - acceleration efficiency

X - focusing efficiency

In formula (5.2) in order to keep E_r constant radius of aperture a have to ^b₁ decreased. So further increase A is limited. In our example design 200 MHz, $W_f = 2.0 \text{ MeV}$, $E_z \rightarrow$ decrease at output end. (See Figs.)

In order to build a short RFQ A must increase, that means more effective high gradient RFQ structure should be invented. (Or chose high rf frequency from view point of view)

The field stabilization in longitudinal direction need more study for four-vane RFQ structure.

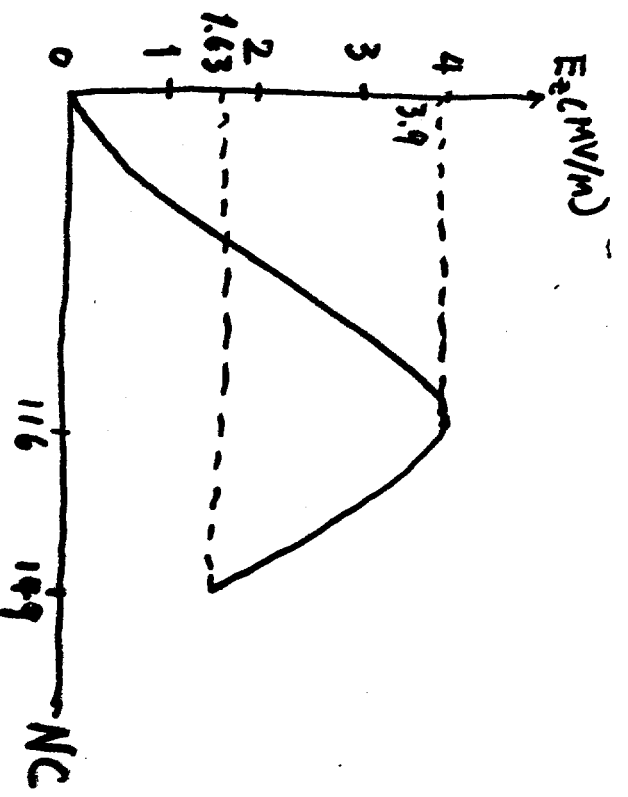
TANK 1 LENGTH= 204.84 CM, 149 CELLS, CHARGE STATE 1.

NC	V	WS	BETA	EZ	CAPA	PHI	A	M	B	CL	TL
60.119	0	0.03000	0.080	0.000	0.00000	-90.0	2.218	1.000	0.572		
100.119	0	0.03000	0.080	0.000	0.00000	-90.0	1.207	1.000	1.530		
200.119	0	0.03000	0.080	0.000	0.00000	-90.0	0.925	1.000	3.289		
300.119	0	0.03000	0.080	0.000	0.00000	-90.0	0.778	1.000	6.596		
400.119	0	0.03000	0.080	0.000	0.00000	-90.0	0.685	1.000	4.647		
500.119	0	0.03000	0.080	0.000	0.00000	-90.0	0.618	1.000	6.596		
600.119	0	0.03000	0.080	0.000	0.00000	-90.0	0.568	1.000	7.354		
700.119	0	0.03000	0.080	0.000	0.00000	-90.0	0.528	1.000	6.596		
800.119	0	0.03000	0.080	0.000	0.00000	-90.0	0.496	1.000	11.440		
900.119	0	0.03000	0.080	0.014	0.00068	-89.9	0.495	1.002	0.596		
1000.119	0	0.03000	0.080	0.027	0.00136	-89.8	0.495	1.005	11.440		
1100.119	0	0.03000	0.080	0.041	0.00205	-89.7	0.494	1.007	11.440		
1200.119	0	0.03000	0.080	0.054	0.00272	-89.7	0.494	1.010	11.441		
1300.119	0	0.03010	0.080	0.058	0.00340	-89.6	0.493	1.012	11.440		
1400.119	0	0.03010	0.080	0.081	0.00408	-89.5	0.492	1.015	11.440		
1500.119	0	0.03010	0.080	0.095	0.00475	-89.4	0.492	1.017	11.440		
1600.119	0	0.03010	0.080	0.108	0.00542	-89.3	0.491	1.020	11.440		
1700.119	0	0.03010	0.080	0.122	0.00609	-89.2	0.491	1.022	11.440		
1800.119	0	0.03010	0.080	0.135	0.00676	-89.1	0.490	1.025	11.440		
1900.119	0	0.03010	0.080	0.148	0.00743	-89.1	0.490	1.027	11.440		
2000.119	0	0.03020	0.080	0.162	0.00810	-88.5	0.489	1.030	11.440		
2100.119	0	0.03020	0.080	0.176	0.00887	-88.9	0.488	1.032	11.440		
2200.119	0	0.03020	0.080	0.188	0.00944	-88.9	0.488	1.034	11.440		
2300.119	0	0.03030	0.080	0.202	0.01011	-88.7	0.487	1.037	11.440		
2400.119	0	0.03030	0.080	0.215	0.01078	-88.8	0.487	1.039	11.440		
2500.119	0	0.03030	0.080	0.228	0.01144	-88.5	0.486	1.042	11.440		
2600.119	0	0.03040	0.080	0.241	0.01211	-88.4	0.486	1.044	11.440		
2700.119	0	0.03040	0.081	0.254	0.01276	-88.4	0.485	1.047	11.440		
2800.119	0	0.03050	0.081	0.267	0.01342	-88.3	0.485	1.049	0.598		
2900.119	0	0.03050	0.081	0.280	0.01408	-88.2	0.484	1.052	11.440		
3000.119	0	0.03060	0.081	0.293	0.01474	-88.1	0.483	1.054	11.440		
3100.119	0	0.03060	0.081	0.306	0.01540	-88.0	0.483	1.056	11.440		
3200.119	0	0.03070	0.081	0.319	0.01607	-87.9	0.482	1.059	11.440		
3300.119	0	0.03080	0.081	0.332	0.01674	-87.8	0.482	1.061	11.440		
3400.119	0	0.03080	0.081	0.345	0.01741	-87.8	0.481	1.064	11.440		
3500.119	0	0.03080	0.081	0.358	0.01809	-87.7	0.481	1.066	11.440		
3600.119	0	0.03100	0.081	0.371	0.01876	-87.6	0.480	1.068	11.440		
3700.119	0	0.03100	0.081	0.384	0.01943	-87.5	0.480	1.071	11.440		
3800.119	0	0.03120	0.082	0.397	0.02018	-87.4	0.479	1.073	11.440		
3900.119	0	0.03130	0.082	0.410	0.02086	-87.3	0.479	1.076	11.440		
4000.119	0	0.03140	0.082	0.424	0.02157	-87.2	0.478	1.078	11.440		
4100.119	0	0.03150	0.082	0.437	0.02228	-87.1	0.478	1.081	11.440		
4200.119	0	0.03160	0.082	0.450	0.02300	-87.1	0.477	1.083	0.603		
4300.119	0	0.03170	0.082	0.463	0.02371	-87.0	0.477	1.083	11.440		
4400.119	0	0.03190	0.082	0.475	0.02432	-86.9	0.476	1.085	11.440		
4500.119	0	0.03200	0.083	0.486	0.02495	-86.8	0.476	1.087	11.440		
4600.119	0	0.03210	0.083	0.497	0.02558	-86.7	0.476	1.089	11.440		
4700.119	0	0.03230	0.083	0.508	0.02623	-86.6	0.475	1.093	11.440		
4800.119	0	0.03250	0.083	0.520	0.02688	-86.5	0.475	1.095	11.440		
4900.119	0	0.03260	0.083	0.532	0.02755	-86.4	0.474	1.097	11.440		
5000.119	0	0.03280	0.084	0.543	0.02822	-86.3	0.474	1.099	11.440		
5100.119	0	0.03300	0.084	0.555	0.02891	-86.3	0.474	1.102	11.440		
5200.119	0	0.03320	0.084	0.567	0.02962	-86.2	0.473	1.104	11.440		
5300.119	0	0.03340	0.084	0.579	0.03033	-86.1	0.473	1.106	11.440		
5400.119	0	0.03360	0.085	0.591	0.03103	-86.0	0.472	1.108	11.440		
5500.119	0	0.03380	0.085	0.603	0.03181	-85.9	0.472	1.110	11.440		
5600.119	0	0.03410	0.085	0.616	0.03257	-85.8	0.472	1.112	11.440		
5700.119	0	0.03430	0.086	0.628	0.03334	-85.7	0.471	1.114	11.440		
5800.119	0	0.03460	0.086	0.641	-85.6	0.471	1.116	11.441	0.631		
5900.119	0	0.03480	0.086	0.654	0.470	1.118	11.441	0.634	35.05		
6000.119	0	0.03495	0.086	0.654	0.470	1.118	11.441	0.636	35.15		

One possibility to build a short RFQ Linac is to increase Kilpatrick limit and use high rf power source to get high field gradient (at TAC) using existing RFQ structure. The other possibility to build a short RFQ Linac is to seek new RFQ structure which has high accelerating eff. meanwhile keeps the focusing strength constant.

N C V W S B E 2 C A P A P H I A M B C L T L

*PARMTEQ result obtained
at Fermilab computer.*



the end of central bunching section

610.119	0	0.3540	0.0087	0.674	0	0.3629	-85.3	0	470	1	121	11.441	0	6.641	36.96	
620.119	0	0.3570	0.0087	0.683	0	0.3693	-85.3	0	470	1	122	11.441	0	6.643	37.61	
630.119	0	0.3600	0.0088	0.692	0	0.3759	-85.2	0	469	1	124	11.441	0	6.646	38.26	
640.119	0	0.3630	0.0088	0	702	0	0.3828	-85.1	0	469	1	125	11.441	0	6.649	38.90
650.119	0	0.3660	0.0088	0	721	0	0.3894	-85.0	0	468	1	126	11.441	0	6.652	39.56
660.119	0	0.3700	0.0089	0.721	0	0.3969	-84.9	0	468	1	127	11.441	0	6.655	40.21	
670.119	0	0.3730	0.0089	0.730	0	0.4037	-84.8	0	468	1	129	11.441	0	6.658	40.87	
680.119	0	0.3770	0.0090	0.740	0	0.4111	-84.7	0	468	1	130	11.441	0	6.661	41.53	
690.119	0	0.3810	0.0090	0.750	0	0.4186	-84.6	0	468	1	131	11.441	0	6.664	42.19	
700.119	0	0.3850	0.0091	0.760	0	0.4254	-84.5	0	467	1	133	11.441	0	6.667	42.86	
710.119	0	0.3880	0.0091	0.770	0	0.4343	-84.4	0	467	1	134	11.441	0	6.671	43.53	
720.119	0	0.3930	0.0092	0.781	0	0.4425	-84.3	0	467	1	136	11.441	0	6.676	44.20	
730.119	0	0.3980	0.0092	0.791	0	0.4505	-84.2	0	467	1	137	11.441	0	6.678	44.88	
740.119	0	0.4020	0.0093	0.802	0	0.4594	-84.1	0	468	1	138	11.441	0	6.682	45.56	
750.119	0	0.4070	0.0093	0.812	0	0.4682	-84.0	0	468	1	140	11.441	0	6.686	46.25	
760.119	0	0.4120	0.0094	0.823	0	0.4778	-83.8	0	468	1	141	11.441	0	6.691	46.94	
770.119	0	0.4170	0.0094	0.832	0	0.4867	-83.1	0	465	1	142	11.441	0	6.696	47.64	
780.119	0	0.4230	0.0095	0.842	0	0.4955	-82.6	0	465	1	147	11.441	0	6.701	48.34	
790.119	0	0.4300	0.0096	0.852	0	0.5052	-82.1	0	465	1	144	11.441	0	6.706	49.04	
800.119	0	0.4370	0.0096	0.862	0	0.5153	-81.6	0	465	1	145	11.441	0	6.711	49.75	
810.119	0	0.4440	0.0097	0.872	0	0.5259	-81.1	0	465	1	146	11.441	0	6.717	50.47	
820.119	0	0.4530	0.0098	0.883	0	0.5371	-80.6	0	464	1	147	11.441	0	6.724	51.19	
830.119	0	0.4620	0.0098	0.894	0	0.5496	-80.1	0	464	1	148	11.441	0	6.731	51.93	
840.119	0	0.4710	0.0100	0.905	0	0.5615	-79.5	0	464	1	149	11.441	0	6.738	52.66	
850.119	0	0.4820	0.0101	0.917	0	0.5746	-79.0	0	463	1	151	11.441	0	6.746	53.41	
860.119	0	0.4930	0.0102	0.928	0	0.5883	-78.5	0	463	1	152	11.441	0	6.754	54.16	
870.119	0	0.5040	0.0104	0.940	0	0.6027	-77.9	0	463	1	153	11.441	0	6.763	54.93	
880.119	0	0.5170	0.0105	0.952	0	0.6178	-77.4	0	463	1	154	11.441	0	6.773	55.70	
890.119	0	0.5310	0.0106	0.964	0	0.6339	-76.8	0	462	1	155	11.441	0	6.782	56.48	
900.119	0	0.5450	0.0108	0.976	0	0.6501	-76.2	0	462	1	157	11.441	0	6.793	57.28	
910.119	0	0.5561	0.0109	0.988	0	0.6672	-75.7	0	462	1	158	11.441	0	6.804	58.08	
920.119	0	0.5670	0.0111	0.999	0	0.6851	-75.1	0	461	1	159	11.441	0	6.816	58.89	
930.119	0	0.5950	0.0113	1.011	0	0.7037	-74.5	0	461	1	160	11.441	0	6.828	59.72	
940.119	0	0.6140	0.0114	1.023	0	0.7220	-73.9	0	461	1	162	11.441	0	6.841	60.56	
950.119	0	0.6340	0.0115	1.047	0	0.7533	-73.9	0	460	1	165	11.441	0	6.856	61.42	
960.119	0	0.6550	0.0118	1.079	0	0.7894	-71.9	0	460	1	169	11.441	0	6.872	62.29	
970.119	0	0.6830	0.0121	1.108	0	0.8267	-70.7	0	460	1	174	11.441	0	6.886	63.18	
980.119	0	0.7110	0.0123	1.139	0	0.8684	-69.5	0	457	1	179	11.441	0	64.98	64.98	
990.119	0	0.7420	0.0128	1.170	0	0.9085	-68.4	0	456	1	184	11.441	0	65.91	65.91	
1000.119	0	0.7760	0.0129	1.200	0	0.9539	-67.2	0	455	1	194	11.441	0	66.95	66.95	
1010.119	0	0.8130	0.0132	1.230	0	0.9969	-65.9	0	454	1	194	11.441	0	66.96	66.96	
1020.119	0	0.8560	0.0135	1.287	0	1.0734	-64.4	0	452	1	204	11.441	0	67.93	67.93	
1030.119	0	0.8940	0.0139	1.344	0	1.1520	-62.9	0	450	1	214	11.441	0	68.93	68.93	
1040.119	0	0.9580	0.0143	1.402	0	1.2358	-61.3	0	448	1	225	11.441	0	69.98	69.98	
1050.119	0	1.0200	0.0147	1.463	0	1.3302	-59.6	0	445	1	237	11.440	0	70.95	71.05	
1060.119	0	1.0910	0.0152	1.550	0	1.4587	-57.8	0	442	1	255	11.440	0	71.92	72.10	
1070.119	0	1.1720	0.0158	1.835	0	1.5908	-55.9	0	438	1	273	11.440	0	73.34	73.34	
1080.119	0	1.2650	0.0164	1.747	0	1.7655	-53.9	0	433	1	299	11.440	0	74.54	74.54	
1090.119	0	1.3750	0.0171	1.887	0	1.9849	-51.8	0	427	1	328	11.440	0	75.79	75.79	
1100.119	0	1.5040	0.0179	2.024	0	2.2243	-49.7	0	420	1	368	11.440	0	76.95	77.10	
1110.119	0	1.6570	0.0188	2.202	0	2.5377	-47.4	0	411	1	418	11.440	0	78.47	78.47	
1120.119	0	1.8410	0.0198	2.419	0	2.9336	-45.1	0	399	1	484	11.440	0	79.92	79.92	
1130.119	0	2.0650	0.0210	2.686	0	3.4420	-42.6	0	384	1	577	11.440	0	81.44	81.44	
1140.119	0	2.3460	0.0223	3.006	0	4.0922	-40.1	0	364	1	709	11.440	0	83.06	83.06	
1150.119	0	2.6840	0.0239	3.426	0	4.9812	-37.5	0	335	1	924	11.440	0	84.79	84.79	
1160.119	0	3.170	0.0258	3.906	0	6.0927	-35.9	0	295	2	272	11.440	1	85.56	86.65	
1170.119	0	4.0830	0.0295	3.717	0	8.1867	-34.8	0	292	2	272	11.440	1	87.31	88.06	
1180.119	0	6.45730	0.0312	3.339	0	6.3042	-34.7	0	291	2	272	11.440	2	82.47	92.99	
1190.119	0	9.50570	0.0328	3.185	0	6.3515	-34.6	0	290	2	272	11.440	2	83.73	95.36	
1200.119	0	12.55840	0.0344	3.050	0	6.33901	-34.5	0	289	2	272	11.440	2	84.93	97.85	
1210.119	0	16.68640	0.0359	2.929	0	6.4221	-34.4	0	288	2	272	11.440	2	85.69	100.46	
1220.119	0	21.65560	0.0374	2.724	0	6.4420	-34.3	0	288	2	272	11.440	2	87.70	103.18	
1230.119	0	27.7710	0.0402	2.635	0	6.4740	-34.2	0	288	2	272	11.440	2	88.94	106.61	
1240.119	0	33.8770	0.0420	2.544	0	6.4919	-34.0	0	287	2	272	11.440	2	89.51	108.94	
1250.119	0	40.03560	0.0446	2.454	0	6.5052	-33.9	0	286	2	272	11.440	2	90.21	111.98	

```

NC V WS BETA E2 CAPA PHI A M B CL TL
1270.119 0.85939 0.8428 2.481 0.05244 -33.8 0.287 2.272 11.440 3.130 115.11
1280.119 0.91070 0.6440 2.412 0.65379 -33.6 0.285 2.272 11.440 3.225 116.33
1290.119 0.86220 0.463 2.349 0.65499 -33.5 0.286 2.272 11.440 3.318 121.65
1300.119 1.01360 0.464 2.291 0.66607 -33.4 0.286 2.272 11.440 3.408 126.68
1306.119 1.06520 0.476 2.230 0.65704 -33.2 0.286 2.272 11.440 3.498 128.68
1320.119 1.11700 0.488 2.185 0.65793 -33.1 0.285 2.272 11.440 3.583 132.13
1330.119 1.16890 0.499 2.138 0.65873 -32.9 0.285 2.272 11.440 3.667 136.89
1340.119 1.22090 0.510 2.093 0.65946 -32.7 0.285 2.272 11.440 3.750 139.56
1350.119 1.27310 0.520 2.050 0.66014 -32.6 0.285 2.272 11.440 3.831 143.38
1360.119 1.32550 0.531 2.011 0.66076 -32.4 0.285 2.272 11.440 3.911 147.29
1370.119 1.37790 0.541 1.973 0.66133 -32.2 0.285 2.272 11.440 3.989 151.28
1380.119 1.43080 0.552 1.937 0.66187 -32.1 0.285 2.272 11.440 4.068 155.35
1390.119 1.48320 0.562 1.903 0.66236 -31.9 0.285 2.272 11.440 4.142 159.49
1400.119 1.53610 0.572 1.871 0.66282 -31.7 0.285 2.272 11.439 4.217 163.71
1410.119 1.58900 0.581 1.840 0.66325 -31.5 0.285 2.272 11.439 4.290 168.00
1420.119 1.64210 0.591 1.810 0.66365 -31.4 0.285 2.272 11.439 4.362 172.36
1430.119 1.69520 0.600 1.782 0.66403 -31.2 0.285 2.272 11.439 4.434 176.79
1440.119 1.74870 0.610 1.755 0.66439 -31.0 0.285 2.272 11.439 4.504 181.36
1450.119 1.80220 0.619 1.730 0.66472 -30.8 0.284 2.272 11.439 4.574 185.87
1460.119 1.85530 0.628 1.705 0.66504 -30.6 0.284 2.272 11.439 4.642 190.51
1470.119 1.90850 0.637 1.681 0.66533 -30.4 0.284 2.272 11.439 4.710 195.22
1480.119 1.96340 0.646 1.658 0.66562 -30.2 0.284 2.272 11.439 4.777 200.60
1490.119 2.01740 0.655 1.636 0.66588 -30.0 0.284 2.272 11.439 4.843 204.84

STOP -1
ELINIT 0.1217
INPUT 8.380 2.76 10.10 0.012505 2.76 10.10 0.012505 180. 0
OUTPUT 3 1 33 56 33 01 1
OUTPUT 2 -1 33 56 00 00 1 500
OUTPUT 2 -1 33 56 00 01 1 500 5
SCHEFF 50.0 0.0497 0.0598 10 20 5 10
BEGIN
END
END
NCCELL = 5, NGOOD = 360
NCCELL = 10, NGOOD = 360
NCCELL = 15, NGOOD = 360
NCCELL = 20, NGOOD = 360
NCCELL = 25, NGOOD = 360
NCCELL = 30, NGOOD = 360
NCCELL = 35, NGOOD = 360
NCCELL = 40, NGOOD = 360
NCCELL = 45, NGOOD = 360
NCCELL = 50, NGOOD = 360
NCCELL = 55, NGOOD = 360
NCCELL = 60, NGOOD = 360
NCCELL = 65, NGOOD = 360
NCCELL = 70, NGOOD = 360
NCCELL = 75, NGOOD = 360
NCCELL = 80, NGOOD = 360
NCCELL = 85, NGOOD = 360
NCCELL = 90, NGOOD = 360
NCCELL = 95, NGOOD = 360
NCCELL = 100, NGOOD = 360
NCCELL = 105, NGOOD = 359
NCCELL = 110, NGOOD = 359
NCCELL = 115, NGOOD = 357
NCCELL = 120, NGOOD = 355
NCCELL = 125, NGOOD = 355
NCCELL = 130, NGOOD = 355
NCCELL = 135, NGOOD = 355
NCCELL = 140, NGOOD = 354
NCCELL = 145, NGOOD = 354
NCCELL = 149, NGOOD = 353
END
OF RUN
0

```

27

RFQSCOPE

BSW-200 RFG

00:57

